Science of the Total Environment 1005 (2025) 180859

Contents lists available at ScienceDirect

Science of the Total Environment

journal homepage: www.elsevier.com/locate/scitotenv

Long-term distribution and vertical migration of plutonium in a peat profile after the 1993 Siberian Chemical Combine accident

Irina E. Vlasova [a,*], Tatiana R. Poliakova [a,b], Andrey S. Toropov [a], Aleksandra V. Rzhevskaia [a], Maria R. Khabarova [a], Vasiliy O. Yapaskurt [c], Anna Yu. Romanchuk [a], Stepan N. Kalmykov [a]

[a] Department of Chemistry, Lomonosov Moscow State University, Moscow, 119991, Russia
[b] MSU-BIT University, Chemistry Department, Shenzhen, 517182, China
[c] Department of Geology, Lomonosov Moscow State University, Moscow, 119991, Russia

HIGHLIGHTS

- Pu remains in low-soluble form in the accidental horizon after 28 years.
- Alpha emitters are concentrated in 'hot' particles in the accidental horizon.
- Vertical migration of Pu through the peat profile has been assumed.
- After 28 years, the maximum levels of ^{137}Cs and ^{241}Am are in the underlying horizon.

GRAPHICAL ABSTRACT

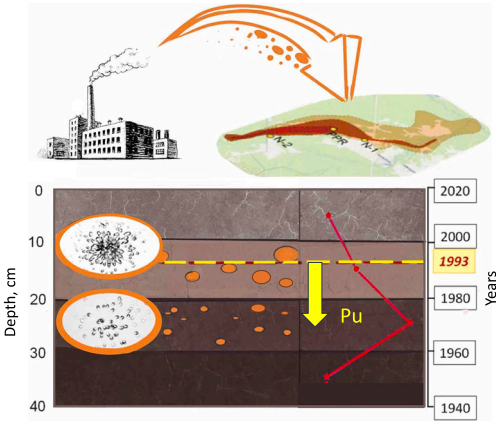

ARTICLE INFO

Keywords:
Plutonium
'Hot' particles
Ombrotrophic Peat
Accidental fallout
Alpha-track radiography
Environmental behavior
Radionuclide migration

ABSTRACT

In 1993, a radiological accident at the Siberian Chemical Combine resulted in a persistent radioactive trace northeast of the Radiochemical Plant, raising long-term concerns about radionuclide mobility in the environment. Among the long-lived radionuclides remaining in soils, plutonium-239 (^{239}Pu) is of particular interest due to its high toxicity and complex environmental behavior. This study determined the distribution and dominant forms of plutonium more than a quarter century after the fallout. A rapidly growing stratified peat bog was subdivided into age horizons based on excess lead-210 (^{210}Pb), which enabled confirmation of vertical migration of plutonium. Alpha Track radiography revealed that over half of the plutonium released during the accident remains trapped within low-solubility 'hot' particles. Data point to the gravitational vertical migration appears to involve small plutonium-bearing particles formed by the degradation of the original fallout material. These

* Corresponding author.
E-mail address: vlasovaie@my.msu.ru (I.E. Vlasova).

https://doi.org/10.1016/j.scitotenv.2025.180859
Received 25 May 2025; Received in revised form 23 September 2025; Accepted 30 October 2025
Available online 4 November 2025

findings emphasize the key role of the initial chemical and physical forms of plutonium in governing its long-term environmental fate.

1. Introduction

On 6 April 1993, at 12:58 p.m. local time, a radiological accident occurred at the Reprocessing Plant of the Siberian Chemical Combine in the Russian Federation (*The Radiological Accident in the Reprocessing Plant at Tomsk,* 1998; Lystsov et al., 1993). An explosion destroyed the first-cycle uranium and plutonium extraction installation, responsible for preparing the initial feedstock for extraction. The affected vessel was a stainless-steel container with a total volume of 34 m^3 and a shell thickness of 14 mm. It was housed in a 4-m-diameter, 7.7-m-deep cell, surrounded by 1.2-m-thick concrete shielding. At the time of the accident, the vessel held 449 g of plutonium (activity: 10^{12} Bq) and 8757 kg of uranium (activity: 1.1×10^{11} Bq), along with β-emitting radionuclides totaling 1.2×10^{14} Bq in activity. The accident was attributed to insufficient compressed air for proper solution mixing, the accumulation of approximately 150 L of organic material, and the presence of degraded solvent. These conditions likely caused the solutions to separate into distinct layers, triggering an autocatalytic, exothermic reaction involving the oxidation and nitration of the organic layer by nitric acid (*The Radiological Accident in the Reprocessing Plant at Tomsk,* 1998; Lystsov et al., 1993; Nosov, 1997; Porfiriev, 1996).

The accident produced a radioactive trace under steady southwest winds (190–210°) at a speed of 8–13 m/s. Radioactive fallout was deposited onto a stable, meter-thick snowpack, which completely melted by mid-May. The trace extended northeast from the Siberian Chemical Combine, deviating eastward about 7 km from the source and turning northward before reaching the village of Georgievka. The axial part of the trace, defined by the 1 μSv/h isoline, stretched for approximately 15 km with a width of about 1 km (Fig. 1). The external gamma dose rate contours were based on aircraft and ground dose rate measurements conducted on 12–13 April along accessible routes at distances of 7–25 km from the accident site. Beta dose rate measurements revealed significant patchiness of contamination, associated with the presence of "hot" particles. Some isolated particles measured 8–10 μm in size and exhibited dose rates up to 220 μSv/h, primarily due to ^{95}Nb (Lystsov et al., 1993). In April–May 1993, 97 % of radioactivity in snow samples collected along the radioactive trace was associated with particulate matter in the melted snow. The significant local heterogeneity of soil contamination was attributed to the presence of "hot" particles with activities up to $n{\cdot}10^5$ Bq per particle, with a density estimated at 400 particles per m^2 near the village of Georgievka (Nosov, 1997).

The most detailed early studies were conducted near Georgievka, the only settlement affected by the fallout and located at the northeastern edge of the trace. The main hazard to the population was due to ^{90}Sr and other β-emitters, which made the main contribution to the dose rate. The contribution of α-emitters was smaller: at the trace margin near Georgievka, ^{239}Pu contamination density ranged from 7.4 to 14.8 MBq/km^2 (Lystsov et al., 1993). The total alpha activity of the contamination was distributed as follows: 0.8 (^{239}Pu): 0.1 (^{234}U): 0.1 (^{238}U). (Lystsov et al., 1993). The fallout trace was spatially restricted, as no evidence of 1993 accident on Siberian Chemical Combine was found in the sedimentary record of Lake Krugloe (Vosel et al., 2019) located only 10 km west of

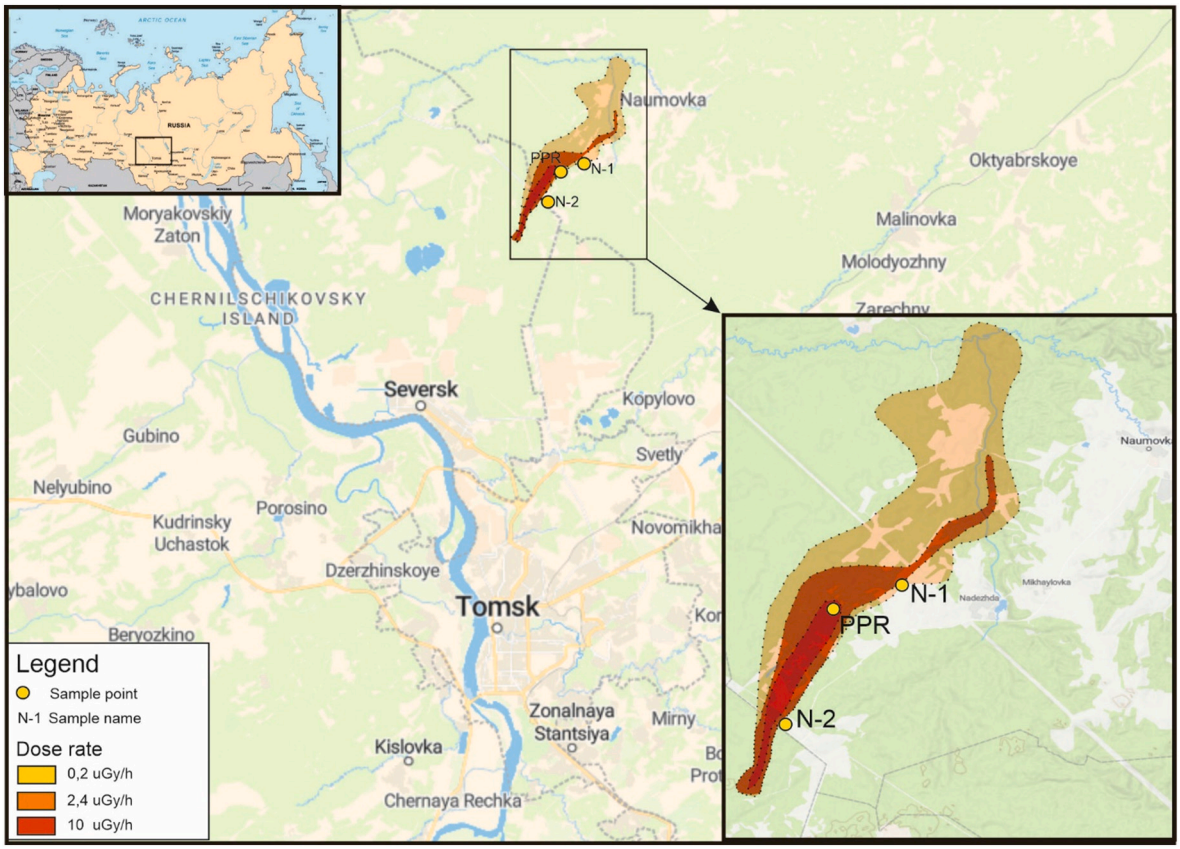

Fig. 1. Sampling locations along the 1993 fallout trace. Contours and dose rate values (μGy h^{-1}) are based on the results of a gamma survey conducted on April 13, 1993, outside the Siberian Chemical Combine (SCC) site (*The Radiological Accident in the Reprocessing Plant at Tomsk,* 1998). The inset in the upper left corner shows the location of the central part of the Tomsk region within northern Asia.

the maximum dose fallout point. Currently, short-lived radionuclides have decayed, and attention has shifted to the migration of long-lived radionuclides, particularly plutonium isotopes. Their importance lies both in their complex chemical behavior and in their toxicity to humans via inhalation or ingestion with drinking water.

The migration behavior of plutonium is complicated by its multiple oxidation states and is influenced by both the characteristics of the plutonium source and geochemical properties and the mineral/organic composition of soils. In the environment, Pu occurs mainly as: (i) sorbed to inorganic phases (Fe/Mn oxyhydroxides, clays), (ii) bound to natural organic matter, (iii) low-solubility PuO_2 'hot' particles, and (iv) dissolved penta- or hexavalent species (Romanchuk et al., 2016). Sorption to inorganic phases and subsequent diffusion are recognized as key mechanisms for its retention. Lysimeter experiments at the Savannah River low-level waste site showed minimal desorption and migration of Pu in vadose sediments, regardless of the initial valence state (III, IV, V). Over 95 % of Pu remained within 1.25 cm of the source after 11 years (Kaplan et al., 2007, 2004, 2010, 2006) and even after aging during 32 years (Emerson et al., 2019). Laboratory studies further demonstrated that PuO_2 nanoparticles formed on Fe oxides and quartz remain stable for months (Powell et al., 2011; Zavarin et al., 2014) and are highly kinetically stable even under acidic conditions (Romanchuk et al., 2013).

Recent studies have highlighted the crucial role of natural organic matter in plutonium mobility (P. Zhao et al., 2011; Santschi et al., 2017; Lin et al., 2019), recognizing its dual role in both immobilizing and mobilizing Pu. Soil organic matter can either correlate with plutonium retention (Kazakevičiūtė-Jakučiūnienė et al., 2021; Xu et al., 2015; Lin et al., 2019) or promote Pu mobility via colloidal transport, as observed at the Nevada Test Site (P. Zhao et al., 2011) and the F-Area of the Savannah River Site (Santschi et al., 2017).

Low-solubility PuO_2 'hot' particles form under high-temperature conditions such as weapons tests, industrial fires, or nuclear accidents. These particles, composed mainly of Pu(IV), are resistant to oxidation and dissolution in the environment. Documented cases include the non-nuclear explosion at Maralinga (Ikeda-Ohno et al., 2016), Rocky Flats (Conradson et al., 2011), and incidents at Thule and Palomares (Lind et al., 2007).

Plutonium transport via inorganic pseudocolloids has been observed near multiple nuclear legacy sites (Kersting and Zavarin, 2011; Novikov et al., 2006). Synthetic PuO_2 colloids have been extensively studied with respect to formation, solubility, aging, stability across pH ranges, and effects of Pu concentration, crystallinity, and initial oxidation state (Walther and Denecke, 2013 and references herein). The relative importance of intrinsic versus pseudocolloidal transport was highlighted in a study of intrinsic PuO_2 colloids and their transformation on clay surfaces (P. Zhao et al., 2020).

Direct speciation of radionuclides in contaminated soils using spectroscopic methods is often limited by low concentrations (Conradson et al., 2011; Novikov et al., 2006). In such cases, radiography and sequential extraction provide valuable information on radionuclide partitioning. Radiography enables assessment of distribution uniformity, identification of localized concentrations ("hot" particles), estimation of their abundance, and quantification of their contribution to total radioactivity (Poliakova et al., 2024). Alpha Track radiography using solid-state detectors has confirmed the presence of 'hot' particles containing α-emitting radionuclides in soils from the 1993 radioactive trace (Tcherkezian et al., 1995; Gromov et al., 1995). Six months after the accident, non-destructive α-track analysis revealed increasing particle abundance closer to the source, with soil α activities ranging from 400 to 1500 Bq kg^{-1} at distances of 7–1 km (Gromov et al., 1995).

For retrospective studies of radionuclide behavior, stratified undisturbed natural archives such as lake sediments (Lin et al., 2019) and ombrotrophic peat bogs (Fiałkiewicz-Kozieł et al., 2025; Cwanek et al., 2021; X. Zhao et al., 2024; Mezhibor et al., 2011; Yakovlev et al., 2021; Testa et al., 1999) are widely used. In most Northern Hemisphere peat profiles, maximum Pu levels generally correspond to 1952 and 1963, linked to global stratospheric fallout before the cessation of atmospheric tests (Fiałkiewicz-Kozieł et al., 2025; Cwanek et al., 2021; X. Zhao et al., 2024). In contrast, Pu profiles in the Tomsk–Seversk region show different maxima and isotope ratios, reflecting contributions from the SCC (Gauthier-Lafaye et al., 2008; Fiałkiewicz-Kozieł et al., 2025).

The ombrotrophic nature of the Petropavlovsky Ryam peatland, hydrologically isolated and fed only by precipitation, has been documented (Gauthier-Lafaye et al., 2008; Mezhibor et al., 2011). Detailed ^{210}Pb dating in 2 cm thick layers confirmed the vertical distribution of Pu isotopes along with the ^{241}Am and ^{137}Cs contents at several SCC-adjacent sites, including the Petropavlovsky Ryam (Gauthier-Lafaye et al., 2008). The role of organic ligands in U and Th binding has also been noted (Toropov et al., 2025).

Our study focuses on the distribution and migration behavior of Pu in soils from the radioactive trace of 1993 accident more than a quarter century after the fallout. We emphasize the identification of mobile and immobile forms of α-emitting radionuclides, particularly Pu, within a stratified, fast-growing peat profile with known age control. To elucidate Pu mobility, we investigate both its vertical distribution across the profile and its microdistribution within individual soil layers, including its association with 'hot' particles.

2. Materials and methods

2.1. Sampling

Three sampling points were selected along the radioactive trace, differing in contamination intensity and soil composition. In August 2019 surface soil samples (up to the depth 5 cm) were collected in two sampling points near the road towards Naumovka village at the location 'N-1' and 'N-2' (Fig. 1). Samples were taken using the "envelope" method to control the spotty fallout and were named 'N-1-1', 'N-1-2', … and 'N-2-1', 'N-2-2'… These two sampling points were located on the East edge of the radioactive trace of the accident 1993 with an initial dose rate of about 1μGy h^{-1}.

In July 2021 the peat core was collected from the active part (up to a depth of 50 cm) of the Petropavlovsky Ryam high-moor peat bog. The sampling point is located in the zone of maximum dose rates of the 1993 accident and is marked on the map as 'PPR' (Fig. 1). Peat sampling was carried out by monolithic extraction through a soil pit to ensure the preservation of vertical stratigraphic integrity and minimize compaction of the peat matrix. This approach is widely used for obtaining undisturbed samples for high-resolution geochemical and paleoecological studies (De Vleeschouwer et al., 2010). A rectangular pit (1.0 × 0.5 m) was excavated to a depth greater than the sampling depth. One vertical wall was cleaned with a stainless-steel knife to prepare a smooth stratigraphic profile. A monolith (0.2 × 0.2 × 0.5 m) was then cut and extracted using a large stainless-steel knife to avoid metal contamination. The peat block was divided into 10 cm layers (P-10, P-20, …, P-50). Each waterlogged layer (3–4 kg) was split vertically into two equal parts for parallel analyses. For the 10–20 cm interval (P-20), one half was further subdivided into 2.5 cm slices to study ^{210}Pb, ^{137}Cs, and Pu isotopes in more detail.

Chronological markers for global fallout (1963) and the 1993 accident were identified based on ^{210}Pb dating and previous stratigraphic studies of the Petropavlovsky Ryam peat (Gauthier-Lafaye et al., 2008; Mezhibor et al., 2011), and our chronological data allowed us to conditionally separate these two main events.

2.2. Analytical methods

Soil and peat samples were air-dried to constant weight and gently disaggregated with a mortar and pestle to a fraction <0.25 mm. Gamma-emitting radionuclides ^{210}Pb, ^{226}Ra, ^{137}Cs, ^{241}Am were measured using γ-spectrometry with a broad energy (from 3 to 10,000 keV)

semiconductor HPGe detector (ORTEC DSPec50, AMETEK). The dried sample weight for gamma spectrometry was 7¬9 g. Each sample was analyzed in duplicate from independently prepared subsamples. Counting time was in a range from 90,000 to 300,000 s. The minimum detectable activities (MDA) for ^{210}Pb and ^{226}Ra, calculated based on counting times ranging from 90,000 to 300,000 s, were achieved as 1¬5 Bq kg^{-1}.

Peat accumulation rates were estimated based on the excess of ^{210}Pb (^{210}Pbex) using ^{210}Pb activity taking into account 226Ra activity and the model of the Constant Rate of Supply (CRS) developed by (Appleby and Oldfield, 1978) was applied. Experimental data for unsupported Pb-210 in the peat profile were fitted by regression model to calculate accumulation rate in given peat cross section. Assuming constant accumulation rate and peat density in upper active layer, a peat accumulation rate of 0.5 cm year^{-1}/ was obtained, which is consistent with published estimates (Gauthier-Lafaye et al., 2008; Mezhibor et al., 2011).

Total Pu activity concentrations in peat and soil samples were determined after autoclave digestion with ultratrace grade acids (HNO_{3conc}: HCl_{conc}: HF_{conc}: H_2O_2) in a ratio 5:1:1:1 for 1.5 h at a temperature of 220 °C using the ETHOS Microwave Digestion System with 1–3 g of dried samples. A ^{236}Pu spike with a known activity was added prior to digestion to control the chemical yield. Therefore, standard post-digestion procedures (removal of HF traces with H_3BO_3, co-precipitation with calcium phosphate and separation on TRU/TEVA resins) followed by (Eichrom Technologies, LLC Method No: ACW17VBS Analytical Procedure Rev. 1.2, 2014). Sources for α-spectrometry were prepared using cerium fluoride microprecipitation and subsequent deposition on Triskem Resolve® membranes. Alpha sources were counted using an ORTEC Alpha-Ensemble-2 spectrometer with an ENS-U900 type UL-TRA-AS α detector having an area of 900 mm^2 (AMETEK). Counting time ranged from 500,000 to 900,000 s. Alternative Pu data were obtained by leaching technique with ignited (450 °C, 6 h) samples with 6 M HCl +7 M HNO_3 under gentle boiling for 1 h, a method widely used for organic matrices samples (e.g. plants and food). Due to incomplete recovery of Pu from peat (particulate-associated radionuclides), these values are reported as “acid-soluble Pu.”

Elemental composition of the mineral fraction of the soils was determined by the XRF (Axios Advanced, PanAnalytical). Trace elements in peat samples determined by ICP-MS (PlasmaQuant MS Elite) Autoclave digestion have been done in the same way as for Pu but with samples weight 0.1–0.5 g. Detection limits for REE, U, Th were 0.1–1 μg kg^{-1}. Ultratrace grade acids and deionized water Milli-Q Millipore, 18.2 MΩ/cm were used for sample preparation. Internal standards for matrix effects and analytical drift correction (103Rh and 193Ir, 50 μg/L, online introduction via a T-connector) supplied.

Soil organic carbon (mentioned as C_{org},) was determined with potassium bichromate-sulfuric acid oxidation and photometric detection with Shimadzu UV-1900i UV–Vis spectrophotometer. Ash content in peat samples was measured as weight loss after drying to constant weight at 105^{0}C and ignition at 450^{0}C for 6 h.

Digital Radiography with Imaging Plate was performed using a Cyclone Storage Phosphor System (PerkinElmer) with SR (super resolution) Imaging Plate and Opti Quant software for scanning and processing images. The image resolution was 600 DPI, the pixel size was 42x42 μm. Separate sample portions of each soil samples were placed in bags to estimate the uniformity of radioactivity distribution. The bags were laid out on a flat substrate and tightly covered with Imaging Plates. The exposure took from 43 to 145 h.

Alpha Track radiography employed with poly-allyl diglycol carbonate detector (MTrack GMScientific Ltd.). Detectors were etched in 6.25M NaOH (80 °C, 4 h) and visualized by optical microscope (Olympus BX-51). Soil sample ‘N-1’ and peat samples taken at different depths were mounted as thin layer on double-sided tape and glued on the glass supports, sized to the α track detectors. Exposition time was 70 days for soil ‘N-1-4’ and up to 41 days for peat samples ‘PPR’. To count α-tracks in the most active clusters in peat bog samples, an additional short exposure of 22 h was performed. The experimental setup and representative examples of α track etch pit images are shown in Fig. 2.

Scanning electron microscopy (JEOL JSM-6480LV with INCA Energy-350) in the back-scattered electron mode was used to search heavy-elements particles and to reveal their morphology and elemental composition.

2.2.1. Quality assurance and quality control (QA/QC)

QA/QC was ensured through the use of standard reference materials, laboratory duplicates, procedural blanks, yield tracers for Pu isotope determination, and regular verification and validation of measuring equipment.

For α-spectrometry, energy calibration was verified with mixed α-sources (238Pu and 241Am), with peak resolution maintained at ≤25 keV FWHM. Counting times were adjusted to achieve relative statistical uncertainty below 10 % (k = 1). Plutonium chemical yields were routinely monitored using a 236Pu spike added prior to solubilization, with recoveries ranging from 43 % to 98 %.

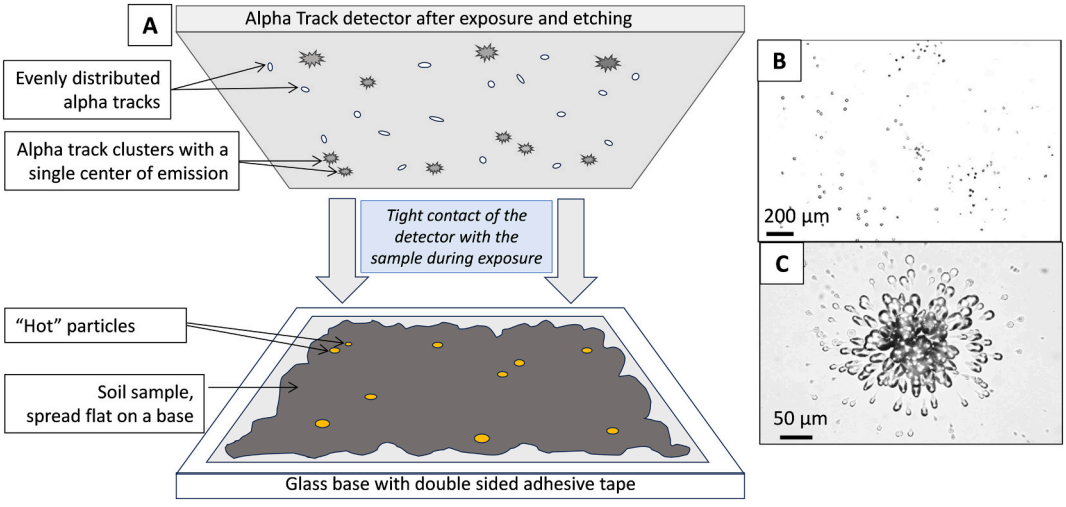

Fig. 2. (A) Experimental design of α-track analysis: following close contact between the α-track detector and the sample preparation, after an exposure period and subsequent etching, evenly distributed multidirectionalαtracks and individual clusters of α tracks originating from single emission centers appear on the detector surface. (B) Example of evenly distributed multidirectional α tracks, corresponding to scattered α activity in the soil sample. (C) Example of an individual cluster of α tracks originating from a single emission center, corresponding to a ‘hot’ particle containing α-emitting radionuclides.

The broad-energy high-purity germanium detector (BEHPGe) for γ-spectrometry was calibrated in energy and efficiency using the IAEA No. 447 multi-nuclide reference material. To ensure analytical quality, the detector efficiency was verified before each measurement series, and background spectra were recorded periodically. Analytical quality was further confirmed through routine measurement of IAEA-447 and in-house organic-matrix reference materials analyzed in identical geometry. Measured activities consistently agreed with certified values.

The laboratory operates under ISO/IEC 17025 accreditation (Russian National Accreditation System), supported by annual internal audits and external assessments. Participation in the IAEA ALMERA proficiency tests for γ-emitting radionuclides demonstrated consistent agreement with certified values for environmental samples.

Trace elements measurements by ICP-MS in peat samples controlled using by BIL-1, Tr-1, LB-1 standards (produced by Vinogradov Institute of Geochemistry SB RAS, Russia) with recovery of trace elements within 87–111 %. were quality-controlled using BIL-1, Tr-1, and LB-1 standards (Vinogradov Institute of Geochemistry SB RAS, Russia), with recoveries of 87–111 %.

2.3. Soil classification and composition

Soil samples 'N-1' and 'N-2' were referred to Luvic Greyzemic Phaeozems and Greyic Phaeozems respectively (World Reference Base for Soil Resources. International Soil Classification System for Naming Soils and Creating Legends for Soil Maps., 2022). These soils are typical for south part of Tomsk region; sampling points landscape is represented by pine forest mixed with wet mossy bogs and small birch groves. All soil samples are very similar to each other in the elemental composition of the mineral part and in the Organic Carbon (C_{org}) concentration (Tables S-1 - S-3). 'N-2' samples differ from 'N-1' in two times lower C_{org} content, as well as low sulfur content - below the detection limit. No technogenic influence was detected either in the main elemental composition or in trace elements in both groups of surface soils ('N-1' and 'N-2').

Peat deposit Petropavlovsky Ryam ('PPR') is the ombrotrophic type of the forest subtype with an atmospheric type of supply with a capacity of up to 2–2.5 m. The botanical composition of Petropavlovsky Ryam peat bog is described in (Mezhibor et al., 2011) and is presented mainly of *Sphagnum magellanicum* and *Sphagnum fuscum*. Table S-3 presents pH values of soils and peat along with C_{org} data for N-1, N-2 samples and ash content for peat samples.

3. Results

3.1. Radioactivity distribution in surface soil samples N-1 and N-2

Data on uranium (U) and thorium (Th) concentrations in soil samples are shown in Figure S-1. In surface soil 'N-1' (average of five samples), mean Th and U concentrations were 4.65 and 2.17 mg·kg^{-1}, respectively. In surface soil 'N-2' (average of three samples), they were 2.45 and 4.01 mg·kg^{-1}. No significant differences were observed between neighboring sampling points (within 20–50 m), and concentrations were within the natural background range for the study area.

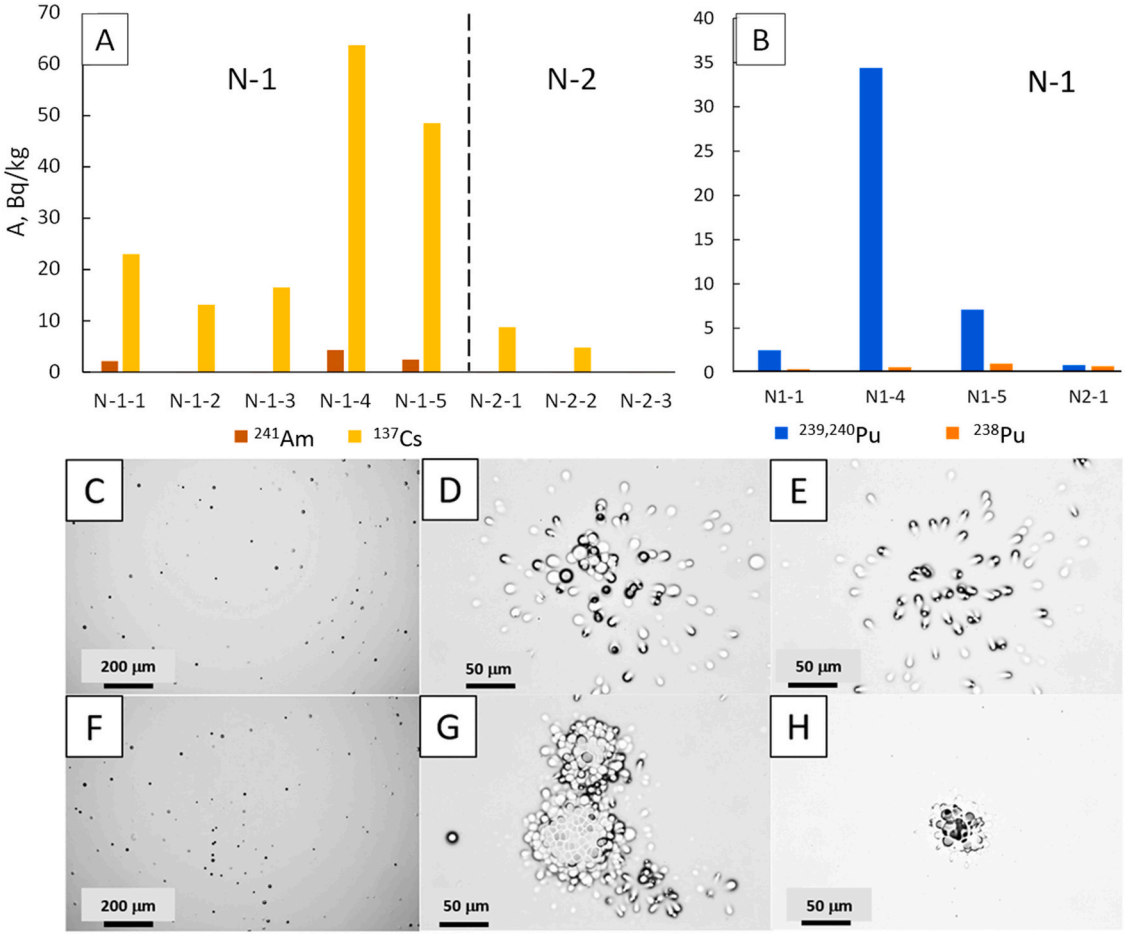

Fig. 3. Radionuclides specific activities and spatial microdistribution of α-emitting nuclides in surface soils 'N-1' and 'N-2' (A) Specific activities of ^{137}Cs and ^{241}Am, Bq kg^{-1}; (B) Specific activity of Pu isotopes, Bq kg^{-1}; (C—H) – examples of α track radiography images of sample N-1-4: (C, F) - evenly distributed α-activity, (D, E, G, H) – clusters of α tracks with a single point of emission, corresponding to "hot" microparticles. Activity values are given as of the date of measurements, for 2019.

At site 'N-1' activity of ^{137}Cs demonstrated pronounced lateral heterogeneity on the meter scale, ranging from 13 to 64 Bq kg^{-1}. ^{241}Am was detected above the limit of detection (LOD) at only three out of five sampling points, with values ranging from 2.2 to 4.3 Bq kg^{-1} (Fig. 3A). In contrast, at site 'N-2' ^{241}Am did not exceed the LOD, and the of activity of ^{137}Cs there were 2–10 times lower than those at site 'N-1'. Based on gamma spectrometry results, samples from the site 'N-2' were excluded from further plutonium measurements as unpromising. Alpha spectrometry of soil samples from site 'N-1' confirmed the data of gamma spectrometry measurements of ^{241}Am and demonstrated the highest ^{239,240}Pu activity values at point N-1-4 (34.4 Bq kg^{-1}, Fig. 3B).

Digital radiography with Imaging Plate of the samples 'N-1' and 'N-2' series showed an excess of photostimulated luminescence signal above background only in sample 'N-1-4'. No noticeable unevenness in radioactivity distribution within the soil sample was observed. Figure S-2 presents a radiogram of a flat preparation of sample 'N-1-4', where the dark gray area corresponds to the soil sample, and the light gray represents the cosmic and other types of background radiation.

Alpha track radiography allowed for extended exposure times without loss of signal quality or significant background interference. Soil sample 'N-1-4', having the highest plutonium content, was selected for detailed study of the α activity micro distribution. A 70-day exposure (27 mg sample, 2.5 cm^2 area) showed that more than 90 % of the detector area is occupied by uniformly distributed α activity (example is presented in Fig. 3 C, F). Dense clusters of α tracks were also observed, corresponding to discrete 'hot' particles (HPs) (Fig. 3 D, E, G, H). These HPs exhibited specific α activities 1–4 orders of magnitude higher than the average uniform background. Rough estimates indicated that ~0.9 $\cdot 10^{-3}$ Bq (about 25 % of the total α activity) was concentrated in 'hot' particles, while 3.2 $\cdot 10^{-3}$ Bq (about 75 %) corresponded to uniformly distributed α activity.

A limitation of surface soil studies, however, is the absence of temporal information on radionuclide dynamics. To better assess long-term Pu migration, a stratified peat profile located within the axial contamination zone was analyzed.

3.2. Peat bog profile: $^{210}Pb_{ex}$ chronology and Peat Accumulation Rate

The measurement of ^{210}Pb activity in the peat profile showed a consistent exponential decrease with depth (Table S-6), justifying the application of a simplified Constant Rate of Supply (CRS) model based on unsupported ^{210}Pb distribution (Appleby and Oldfield, 1978). This model is considered reliable for age intervals of several years and was previously applied for dating the peat profile of Petropavlovsky Ryam deposit (Gauthier-Lafaye et al., 2008). Peat chronology based on measured $^{210}Pb_{ex}$ and CRS dating model confirmed that peat has accumulated at an average rate accumulation of 0.50 cm per year consistent with earlier estimates of dating for the upper 30 cm in the range of 0.47–0.53 cm year^{-1} (Gauthier-Lafaye et al., 2008). In the 14 years since those measurements, the peat growth estimated as 6–7 cm, which is confirmed both ^{210}Pb dating and the coincidence of the Pu peaks. Furthermore, similar rates of peat accumulation rate have been found in the peat deposit very close to Petropavlovsky Ryam, 2 km northwest of Tomsk city - from 0.4 to 1.2 cm year^{-1}, with an average of 0.53 cm/year (Fiałkiewicz-Kozieł et al., 2025). The ^{210}Pb derived chronology is independently supported by the global fallout peak of ^{137}Cs observed in 20–30 cm layer.

Based on this chronology data, a 10-cm-thick core section corresponds to approximately 20 years of accumulation. Consequently, the depth corresponding to the 1993 accident was estimated at 12–14 cm, while the maximum fallout from global atmospheric nuclear testing (circa 1963) was identified at 25–28 cm depth.

3.3. Uranium and thorium concentration and ash content in peat profile

The concentrations of Th and U in the peat profile ranged from 0.2 to 1.2 mg·kg^{-1}and from 0.3 to 1.3 mg·kg^{-1}, respectively. Vertical variations in U and Th concentrations correlated both with each other and with the ash content of peat samples (Table 1). The highest ash content was observed in the 30–40 cm layer, which dates back to the mid-20th century. During this period, the likely main source of dust loading was urban construction activities in the city of Seversk. The contents of U and Th, as well as their ratio, do not reliably indicate anthropogenic input of U into the peat deposit. Comparison of Th and U concentrations in the peat profile with those in surface soils 'N-1' and 'N-2' (Figure S-1) confirmed a correlation between Th and U concentrations and the proportion of the mineral fraction in the soils.

3.4. Vertical distribution of artificial radionuclides in the peat core

Results of γ spectrometry measurements of ^{137}Cs and ^{241}Am, and α spectrometry measurements for total ^{239,240}Pu and the acid-soluble fraction of ^{239,240}Pu in the horizons of the peat core are summarized in Fig. 4 B-E and Tables S-4, S-5. Vertical distributions of radionuclides along the peat profile were measured at 10 cm intervals, averaging radionuclide data over 20-year peat accumulation periods. In the second horizon, 10–20 cm deep, corresponding to the period of the 1993 accident, higher-resolution sampling was carried out at 2.5 cm intervals: 10.0–12.5 cm; 12.5–15.0 cm; 15.0–17.5 cm; and 17.5–20.0 cm.

All studied radionuclides exhibited broadly similar vertical distributions across the peat profile. Maximum specific activities of ^{137}Cs, ^{241}Am and ^{239,240}Pu were observed in the 20–30 cm layer, corresponding to the 1960–1980 period. Relative to the 10–20 cm horizon (1993 fallout), ^{241}Am activity was ~5 times higher, ^{137}Cs about ~3 times higher, acid-soluble ^{239,240}Pu ~ 2 times higher and total ^{239,240}Pu ~ 4 times higher (Fig. 4 B-E). However, an anomalously high total Pu activity was recorded in sample P-20 (1015 and 2080 Bq kg^{-1} (table S-5).This peak is supported by Alpha Tracking radiography data and likely reflects heterogeneous deposition of Pu-containing "hot" particles rather than a gross analytical error. Comparable values were reported by Gromov et al. (Gromov et al., 1995), where α-track studies yielded activities of ~1500 Bq kg^{-1}at the most contaminated sites.

The anomalous Pu values from sample P-20 were excluded from calculation of the mean total Pu activity for this horizon. Repeated measurements of the bulk P-20 sample and its four sublayers yielded more typical Pu activities of 25–40 Bq kg^{-1} (Tables S-4, S-5).

3.5. Alpha track radiography of Petropavlovsky Ryam peat profile samples

Alpha Track radiography of the peat profile confirmed a highly uneven distribution of α-emitting radionuclides within individual layers. Against a background of uniformly distributed multidirectional α tracks, numerous clusters of α tracks originating from single emission centers were observed (Fig. 2 B, C; Table S-7; Figures S-3 – S-21). The uniform tracks represent diffusely distributed α emitters, whereas the clustered tracks indicate discrete 'hot' particles.

This method enables quantitative assessment of α-emitter activity, providing information on both the dispersed fraction and concentrated "hot" particles. For particles with high specific α activity, overlapping tracks complicate counting; to resolve this, multiple exposures of different durations were performed on the same preparation. Examples

Table 1
Thorium and Uranium concentration and ash content of peat bog samples.

Sample	Depth, cm	Th, mg·kg^{-1}	U, mg·kg^{-1}	Ash, %
P-10	0–10	0.25	0.31	6.8
P-20	10–20	0.38	0.45	6.6
P-30	20–30	0.9	0.58	9.1
P-40	30–40	**1.17**	**1.27**	**13.1**
P-50	40–50	0.74	0.65	9.8

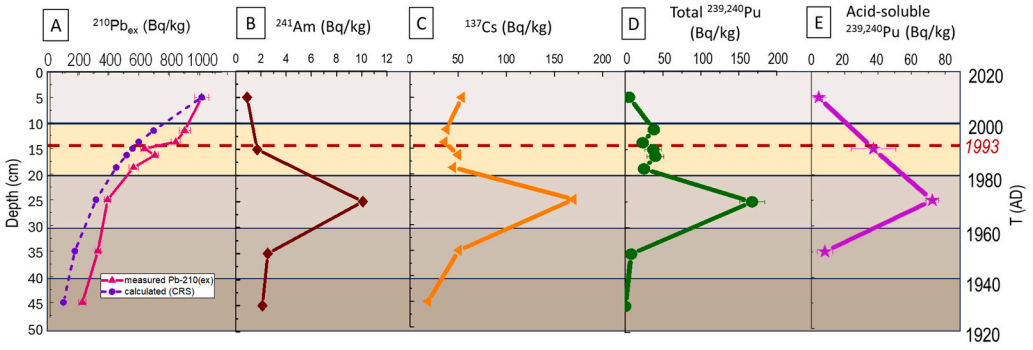

Fig. 4. Peat profile characteristics. (A) ^{210}Pb activity (Bq kg^{-1}) and age model based on Constant Rate of Supply (CRS) approach (5.0 mm $year^{-1}$); (B) ^{241}Am activity (Bq kg^{-1}); (C) ^{137}Cs activity (Bq kg^{-1}), as measured in 2021; (D) total $^{239,240}Pu$ activity (Bq kg^{-1}); (E) acid-soluble fraction of $^{239,240}Pu$ (Bq kg^{-1}).

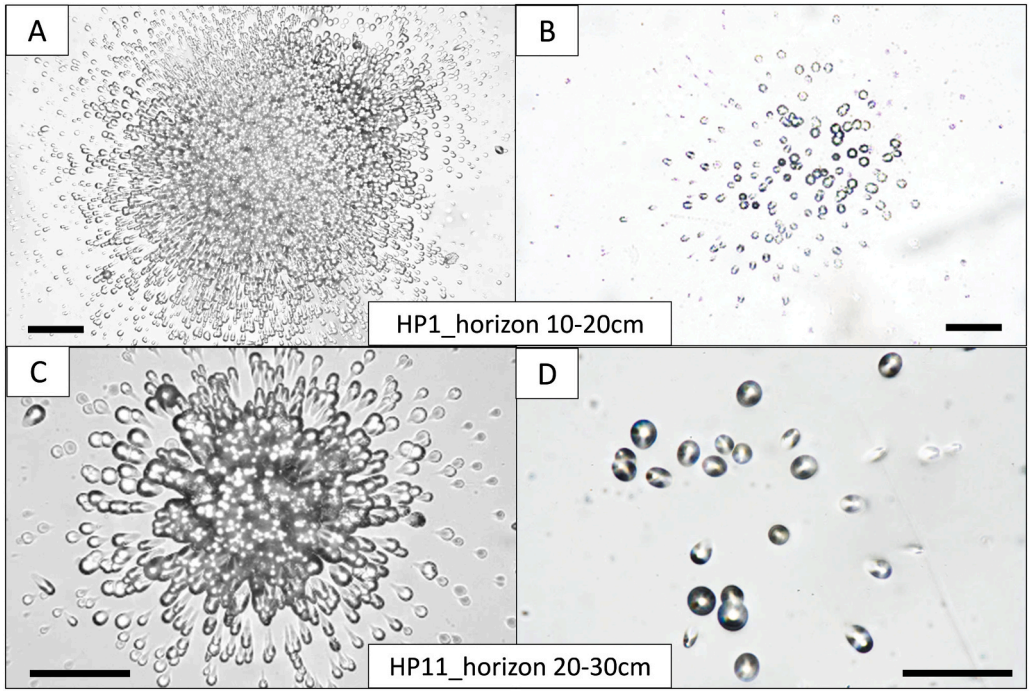

Fig. 5. Alpha Track images of two α -emitting microparticles exposed for different durations: HP1 from 10 to 20 cm layer (A,B); and HP11 from the 20–30 cm layer (C, D); different exposure time: 41 days (A, C) and 22 h (B, D). The scale bar corresponds to 100 μm.

for two microparticles are shown in Fig. 5. This approach allowed determination of both low-activity dispersed emitters and highly active particles. To ensure comparability, results were normalized to sample mass, area, and exposure time.

From α-track analysis, three parameters were calculated:

1. Specific number of dispersed α tracks per unit area or mass per exposure time;
2. Specific number of track clusters from single emission centers ("hot" particles) per unit area or mass;
3. Number of α tracks within "hot" particles per exposure time.

The sum of (1) and (3) represents total α activity (track counts), while the ratio of (3) to the total gives the fraction of α activity in "hot" particles (HP_{fr}).

The vertical distribution of α emitters varied markedly. The lowest densities of "hot" particles were found in the 0–10 cm and 30–40 cm horizons (0.28 and 0.20 mg^{-1}, respectively). Fig. 6A compares the density of "hot" particles in each horizon with HP_{fr} values. The lowest HP_{fr} (2 %) occurred in the uppermost layer, while the highest (78 %) was observed in the 10–20 cm horizon. HP_{fr} values in the 20–30 cm and 30–40 cm horizons were 43 % and 15 %, respectively. The elevated HP_{fr} at 10–20 cm, corresponding to the 1993 fallout, matches expectations.

Interestingly, the density of "hot" particles was higher in the 20–30 cm horizon than in the 10–20 cm horizon. This may reflect post-depositional processes: over the 28 years since the accident, some fallout particles likely underwent dissolution or fragmentation, with smaller fragments migrating downward. As a result, particle numbers increased, but their lower specific activities reduced their relative contribution to total α activity compared with the original fallout layer.

3.6. *Uranium containing particles*

Peat samples from areas showing α-track clusters were further examined by scanning electron microscopy in backscattered electron mode (SEM-BSE) to identify 'hot' particles. Among several dozen analyzed areas corresponding to α-track clusters (Figures S-3, S-7 – S-17, S-19), only three uranium-containing particles were found (Fig. 7): one particle in the second horizon P-20 (10–20 cm) and two particles in the third horizon P-30 (20–30 cm). Most α-track clusters not confirmed by

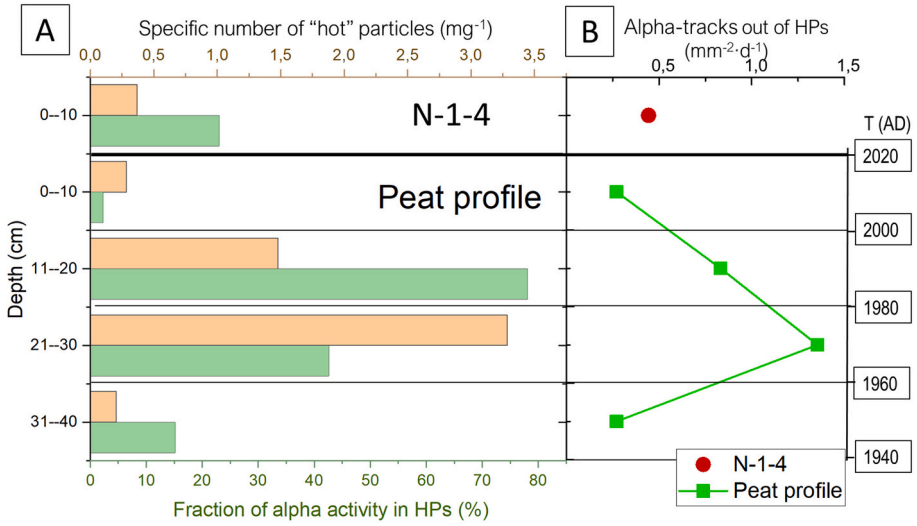

Fig. 6. Alpha Track Analysis of surface soil sample N-1-4 and Petropavlovsky Ryam peat profile samples. (A) - Fraction of α-radioactivity trapped in "hot" particles (green) and specific number of "hot" particles per mg of soil sample (orange). (B) Alpha activity in dispersed form: number of α tracks detected outside "hot" particles per mm^2 of sample per day of exposure.

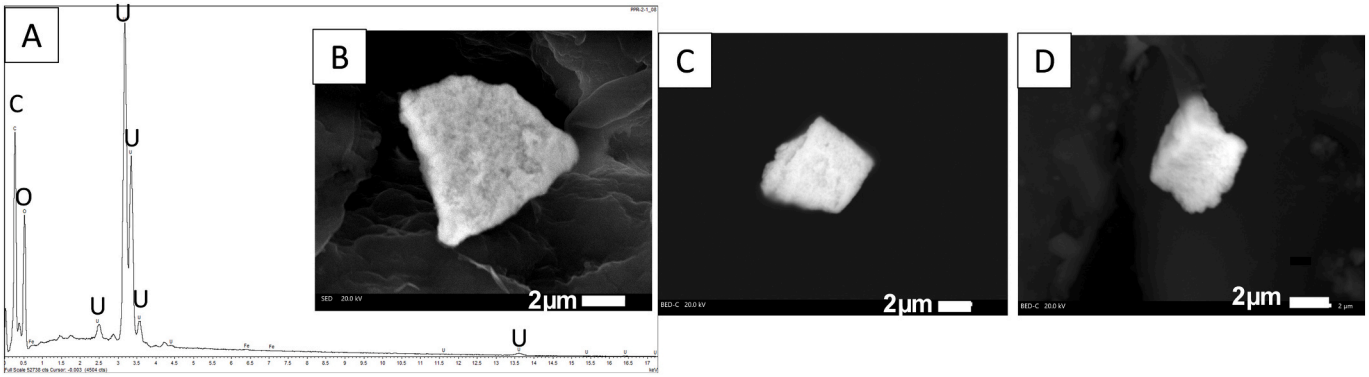

Fig. 7. EDX spectrum (A) and SEM-BSE images (B—D) of uranium-containing particles from peat horizons 10–20 cm (A, B) and 20–30 cm (C, D).

SEM-EDX likely correspond to α-emitting radionuclides with much shorter half-lives than uranium, resulting in very low elemental concentrations below SEM detection limits. In the context of the 1993 fallout, these undetected particles can be confidently attributed mainly to Pu.

4. Discussion

4.1. Stability of plutonium-containing 'hot' particles and lateral distribution of plutonium

Alpha-track radiography demonstrated that plutonium in the accidental horizon predominantly occurs in the form of particles, with a large number of smaller particles also present in the underlying layer. The persistence of plutonium-containing 'hot' particles for more than a quarter of a century, given that the source of radioactive contamination was liquid waste, deserves particular attention. Most of the plutonium has remained in a poorly soluble form under the specific conditions of a peat bog: a water-saturated environment rich in natural organic matter, with a pH of about 5.

The absence of detectable particles in areas with dense α-track clusters, despite thorough SEM characterization, may suggest that these particles are nanoscale in size and that plutonium concentrations are below the SEM detection limit. It remains uncertain whether these particles should be classified as intrinsic colloids or pseudo-colloids. Nucleation of plutonium nanoparticles might even have started within the original extraction installation before the accident. According to meteorological data, the radioactive release coincided with snowfall, which could have promoted the settling of particles on the snowpack. Previous studies have shown that plutonium dioxide particles formed under acidic conditions exhibit enhanced stability (P. Zhao et al., 2020; Tasi et al., 2018).

Marked lateral variability in plutonium concentrations at the meter scale was observed at the edge of the radioactive trace (site 'N-1'). The ^{239}Pu content varied by a factor of 5–10, with the highest value recorded in sample 'N-1-4', coinciding with the lateral distribution of ^{137}Cs. Similar patchiness in the lateral distribution of γ-emitting nuclides was reported shortly after the accident in the same sampling area (near the road Georgievka - Naumovka) and was attributed to aerosol deposition in the form of individual particles, predominantly containing ^{95}Nb and ^{106}Ru at that time (Nosov, 1997). It is therefore reasonable to assume that plutonium was also deposited as individual particles during the fallout.

In sample N-1-4, selected for detailed analysis, we observed pronounced heterogeneity in the microdistribution of α emitters at scales ranging from millimeters to microns. Soon after the accident, Tcherkezian, Gromov, and co-authors (Tcherkezian et al., 1995; Gromov et al., 1995) reported similar extreme micro-scale heterogeneity of α emitters, with spots of 10–100 μm in size, where α activity exceeded the sample average by factors 100–1000. However, those early studies did not

quantify the fraction of radioactivity contained within 'hot' particles.

According to our data, in soil sample 'N-1-4' (located at the trace edge), approximately 25 % of the total α activity was associated with 'hot' particles. In peat soils located within the axial part of the radioactive trace, this value ranged from 15 % (in the 30–40 cm layer) to 78 % (in the 10–20 cm layer). The uneven Pu activity distribution within the accidental horizon, with several anomalous values in peat monoliths (20 × 20 cm) exceeding the mean by one to two orders of magnitude, confirms that Pu was deposited in the form of microparticles.

4.2. Vertical migration of Plutonium under peatland environment

Across the Northern Hemisphere, numerous studies report that plutonium activity in the global fallout horizon of peat profiles is typically ranges between 10 and 25 Bq kg^{-1}(Fiałkiewicz-Kozieł et al., 2025; Cwanek et al., 2021). In contrast, our measurements of ^{239,240}Pu activity in the 20–30 cm peat horizon, corresponding to the global fallout level, were much higher, reaching 167 Bq kg^{-1} (acid-soluble Pu: 72 Bq kg^{-1}). Together with the relatively low ^{238}Pu/^{239,240}Pu isotopic ratio (0.017 ± 0.002 compared with 0.025–0.040 for global fallout), this indicates a different origin of Pu, clearly not from global fallout. Importantly, the isotopic ratio ^{238}Pu/^{239,240}Pu in both the accident horizon (10–20 cm) and the underlying horizon (20–30 cm) remained within a narrow range of 0.014 ± 0.002, pointing to a single source, most likely aerosol fallout from the Siberian Chemical Combine. Considering the only recorded release beyond the enterprise boundaries—the 1993 accident—the elevated Pu activity in the 20–30 cm layer can be explained by downward migration from the accident horizon.

Most peat profiles show no evidence of significant vertical migration of global fallout Pu (Fiałkiewicz-Kozieł et al., 2025; Cwanek et al., 2021; X. Zhao et al., 2024) with rare exceptions (Quinto et al., 2013; Mróz et al., 2017). However, Pu behavior strongly depends on its origin: global versus accidental fallout. Vertical redistribution of Pu from the Chernobyl accident has been demonstrated in several studies (Bossew et al., 2004; Orzeł and Komosa, 2014)), with gradual dissolution of fuel particles driving the release and downward migration of associated radionuclides (Kashparov et al., 2009). A key feature of accidental fallout is the dual occurrence of Pu in dissolved and particulate forms. Over time, Pu-containing microparticles disintegrate into smaller fragments that can percolate to deeper horizons under gravity and subsequently dissolve due to their increased surface area. The fragmentation of large radioactive particles following the 1993 accident was documented by Tcherkezian et al. (Tcherkezian et al., 1995), who reported that 'hot' particles as large as 120 × 200 μm could break down into ~25 smaller particles of ~10 μm.

Our Alpha Track radiography data confirm this process. In the accident horizon (10–20 cm) of the Petropavlovsky Ryam peat profile, approximately 80 % of the α activity is associated with 'hot' particles. In contrast, in the underlying horizon (20–30 cm; 1960–1980), diffuse α-emitters dominate over α activity bound in 'hot' particles (Fig. 6). This suggests that soluble Pu and Pu associated with small particles migrated from the 1993 horizon (~13 cm depth) to the 20–30 cm horizon, corresponding to a vertical displacement of at least ~8 cm. The primary mechanism for Pu mobilization and migration is the complexation with organic ligands that enhance solubility and transport (Wasserman et al., 2023; Sokolik et al., 2004).

4.3. U and Th concentration

Uranium and thorium contents in soil and peat samples correlate with the mineral component fraction. In the peat profile, maximum U and Th concentrations coincided with the maximum ash content and corresponded to the 1940–1960 period, likely associated with increased dust loading during construction activities in Seversk. The U and Th concentrations do not exceed natural background levels. However, we cannot completely exclude a minor anthropogenic contribution of uranium, particularly given the detection of uranium microparticles by SEM-EDX analysis. Nevertheless, this contribution appears insignificant compared to background uranium levels in neighboring areas unaffected by the accident trace (Gedeonov et al., 2009).

5. Conclusions

1. More than a quarter of a century after the accident, the lateral distribution of plutonium isotopes and other radionuclides remains highly heterogeneous, consistent with initial post-event observations. The peat horizon directly affected by the 1993 accidental fallout (10–20 cm) contains anomalous, spotty values with Pu activity reaching thousands of Bq kg^{-1}, exceeding mean values in peat layer by orders of magnitude. The highest activities of ^{137}Cs and ^{241}Am in the peat horizon (20–30 cm), far surpassing typical levels attributable to global fallout in the region.
2. The Pu activity in peat horizon corresponding to 1960–1980 yy (20–30 cm) significantly exceeds the Northern Hemisphere's global fallout levels. The ^{238}Pu/^{239,240}Pu isotope ratio in this horizon deviates from the published range for global fallout, providing clear evidence of the accidental source. The data suggest vertical gravitational migration of Pu containing particles within the peat profile from the initially contaminated horizon to the underlying layers.
3. The physicochemical forms of plutonium differ fundamentally between the studied horizons. In the underlying horizon (20–30 cm), plutonium is predominantly present in a dispersed, acid-soluble form, likely associated with organic matter. In contrast, within the 1993 accident affected horizon, the majority of plutonium (~80 %) remains in poorly soluble particulate forms. These finding highlights that for the accurate determination of Pu activity in such accident-affected samples, a complete digestion pretreatment, including the use of hydrofluoric acid, is essential.
4. The concentrations of uranium and thorium in soil samples from the radioactive trace are generally consistent with regional background levels found outside the accident-affected area. However, the presence of individual uranium (hydro)oxide particles in the 10–20 cm and 20–30 cm horizons localized technogenic uranium contribution cannot be entirely excluded.

CRediT authorship contribution statement

Irina E. Vlasova: Writing – original draft, Methodology, Investigation, Conceptualization. **Tatiana R. Poliakova:** Writing – original draft, Methodology, Investigation. **Andrey S. Toropov:** Writing – review & editing, Resources, Methodology, Investigation. **Aleksandra V. Rzhevskaia:** Investigation. **Maria R. Khabarova:** Investigation. **Vasiliy O. Yapaskurt:** Investigation. **Anna Yu. Romanchuk:** Writing – review & editing, Resources, Methodology. **Stepan N. Kalmykov:** Supervision.

Declaration of competing interest

The authors declare that they have no known competing financial interests or personal relationships that could have appeared to influence the work reported in this paper.

Acknowledgments

The authors are grateful to Sergey Arbuzov (Tomsk Polytechnic University) for assistance in sampling and useful consultations. The work was carried out with the support of the Russian Science Foundation (grant No.19-73-20051) and MSU Development Program (α-spectrometry, γ-spectrometry and ICP-MS).

Appendix A. Supplementary data

Supplementary data to this article can be found online at https://doi.

org/10.1016/j.scitotenv.2025.180859.

Data availability

Data will be made available on request.

References

Appleby, P.G., Oldfield, F., 1978. The Calculation of Lead-210 Dates Assuming a Constant Rate of Supply of Unsupported 210Pb to the Sediment. Catena 5 (1), 1–8. https://doi.org/10.1016/S0341-8162(78)80002-2.

Bossew, Peter, Gastberger, Michael, Gohla, Herbert, Hofer, Peter, Hubmer, Alexander, 2004. Vertical Distribution of Radionuclides in Soil of a Grassland Site in Chernobyl Exclusion Zone. J. Environ. Radioact. 73, 87–99. https://doi.org/10.1016/j.jenvrad.2003.08.004.

Conradson, Steven D., Clark, David L., Den Auwer, Christophe, Lezama-pacheco, Juan S., 2011. Actinide Nanoparticle Research, pp. 377–398. https://doi.org/10.1007/978-3-642-11432-8.

Cwanek, Anna, Łokas, Edyta, Mitchell, Edward A.D., Mazei, Yuri, Gaca, Paweł, Milton, James A., 2021. Temporal Variability of Pu Signatures in a 210Pb-Dated Sphagnum Peat Profile from the Northern Ural, Russian Federation. Chemosphere 281, 130962. https://doi.org/10.1016/j.chemosphere.2021.130962.

Vleeschouwer, F. De, Chambers, F.M., Swindles, G.T., 2010. Coring and Sub-Sampling of Peatlands for Palaeoenvironmental Research. Mires and Peat 7, 1–10.

Emerson, Hilary P., Kaplan, Daniel I., Powell, Brian A., 2019. Plutonium Binding Affinity to Sediments Increases with Contact Time. Chem. Geol. 505, 100–107. https://doi.org/10.1016/j.chemgeo.2018.11.009.

Fiałkiewicz-Kozieł, Barbara, Smieja-Kro'l, Beata, Edyta, Łokas, Cwanek, Anna, Plado, Jüri, Mr'oz, Tomasz, Wąsowicz, Paweł, Gałka, Mariusz, 2025. Synchronizing Pu fallout and inorganic fly ash particles record in Northern Hemisphere peatlands. Sci. Total Environ. 993, 180011. https://doi.org/10.1016/j.scitotenv.2025.180011.

Gauthier-Lafaye, F., Pourcelot, L., Eikenberg, J., Beer, H., Le Roux, G., Rhikvanov, L.P., Stille, P., Renaud, Ph., Mezhibor, A., 2008. Radioisotope Contaminations from Releases of the Tomsk-Seversk Nuclear Facility (Siberia, Russia). J. Environ. Radioact. 99 (4), 680–693. https://doi.org/10.1016/j.jenvrad.2007.09.008.

Gedeonov, A.D., Kolchin, I.V., Malishkin, A.I., Andreev, G.S., 2009. Uranium-234, Uranium-235 and Uranium-238 in Soil near Siberian Chemical Enterprises (Tomsk-7, Seversk). Radioprotection 44 (5), 151–153. https://doi.org/10.1051/radiopro/20095032.

Gromov, A.V., Nikolaev, V.A., Andreev, G.S., 1995. An Assessment by the Track Method of Soil Alpha-Activity near the City of Tomsk. Radiat. Meas. 25 (1–4), 395–396. https://doi.org/10.1016/1350-4487(95)00125-X.

Ikeda-Ohno, Atsushi, Lida Mokhber Shahin, Daryl L. Howard, Richard N. Collins, Timothy E. Payne, Mathew P. Johansen, 2016. Fate of Plutonium at a former nuclear testing site in Australia. Environ. Sci. Technol. 50 (17), 9098–9104. https://doi.org/10.1021/acs.est.6b01864.

Kaplan, Daniel I., Powell, Brian A., Demirkanli, Deniz I., Fjeld, Robert A., Molz, Fred J., Serkiz, Steven M., Coates, John T., 2004. Influence of oxidation states on plutonium mobility during long-term transport through an unsaturated subsurface environment. Environ. Sci. Technol. 38 (19), 5053–5058. https://doi.org/10.1021/es049406s.

Kaplan, Daniel I., Demirkanli, Deniz I., Gumapas, Leo, Powell, Brian A., Fjeld, Robert A., Molz, Fred J., Serkiz, Steven M., 2006. Eleven-year field study of Pu migration from Pu III, IV, and VI sources. Environ. Sci. Technol. 40 (2), 443–448. https://doi.org/10.1021/es050073o.

Kaplan, Daniel I., Powell, Brian A., Duff, Martine C., Demirkanli, Deniz I., Denham, Miles, Fjeld, Robert A., Molz, Fred J., 2007. Influence of sources on plutonium mobility and oxidation state transformations in vadose zone sediments. Environ. Sci. Technol. 41 (21), 7417–7423. https://doi.org/10.1021/es0706302.

Kaplan, Demirkanli, F J Molz, D M Beals, J R Cadieux, Jr, J E Halverson, 2010. Upward movement of Plutonium to surface sediments during an 11-year field study. J. Environ. Radioact. 101 (5), 338–344. https://doi.org/10.1016/j.jenvrad.2010.01.007.

Kashparov, Valery, Ahamdach, Noureddine, Levchuk, Svyatoslav, Yoschenko, Vasyl, Fesenko, Sergey, Maloshtan, Igore, 2009. Dissolution of Particles of Irradiated Nuclear Fuel in the Temporary Storages of Radioactive Waste in Chernobyl Zone: Sources for Radionuclide Migration. In: Radioactive Particles in the Environment, pp. 139–156.

Kazakevičiūtė-Jakučiūnienė, Laima, Druteikienė, Rūta, Maceika, Evaldas, Lukšienė, Benedikta, Juškėnas, Remigijus, Pakštas, Vidas, Žukauskaitė, Zita, Gvozdaitė, Rasa, Tarasiuk, Nikolaj, 2021. Impact of Soil Organic Matter on Pu Migration in Five Lithuanian Surface Soils. J. Environ. Radioact. 237, 106702. https://doi.org/10.1016/j.jenvrad.2021.106702.

Kersting, Annie B., Zavarin, Mavrik, 2011. Actinide Nanoparticle Research. https://doi.org/10.1007/978-3-642-11432-8.

Lin, Peng, Chen, Xu, Kaplan, Daniel I., Chen, Hongmei, Yeager, Chris M., Xing, Wei, Sun, Luni, et al., 2019. Nagasaki sediments reveal that long-term fate of plutonium is controlled by select organic matter moieties. Sci. Total Environ. 678, 409–418. https://doi.org/10.1016/j.scitotenv.2019.04.375.

Lind, O.C., Salbu, B., Janssens, K., Proost, K., García-León, M., García-Tenorio, R., 2007. Characterization of U/Pu Particles Originating from the Nuclear Weapon Accidents at Palomares, Spain, 1966 and Thule, Greenland, 1968. Sci. Total Environ. 376 (1–3), 294–305. https://doi.org/10.1016/j.scitotenv.2006.11.050.

Lystsov, V.N., Ivanov, A.B., Kolyshkin, A.E., 1993. Radioecological Aspects of the Accident in Tomsk. Atomic Energy 74 (4), 367–369.

Mezhibor, Antonina, Arbuzov, Sergey, Rikhvanov, Leonid, Gauthier-Lafaye, Francois, 2011. History of the Pollution in Tomsk Region (Siberia, Russia) According to the Study of High-Moor Peat Formations. Int. J. Geosci. 02 (04), 493–501. https://doi.org/10.4236/ijg.2011.24052.

Mróz, Tomasz, Łokas, Edyta, Kocurek, Justyna, Gąsiorek, Michał, 2017. Atmospheric Fallout Radionuclides in Peatland from Southern Poland. J. Environ. Radioact. 175–176, 25–33. https://doi.org/10.1016/j.jenvrad.2017.04.012.

Nosov, A.V., 1997. Investigation of the State of River System in the Seversk Region after the Radiation Accident at the Siberian Chemical Plant on April 6, 1993. At. Energy 83 (1), 526–530.

Novikov, Alexander P., Kalmykov, Stepan N., Utsunomiya, Satoshi, Ewing, Rodney C., Horreard, François, Merkulov, Alex, Clark, Sue B., Tkachev, Vladimir V., Myasoedov, Boris F., 2006. Colloid transport of Plutonium in the far-field of the Mayak Production Association, Russia. Science 314 (5799), 638–641. https://doi.org/10.1126/science.1131307.

Orzeł, Jolanta, Komosa, Andrzej, 2014. Study on the rate of plutonium vertical migration in various soil types of Lublin region (Eastern Poland). J. Radioanal. Nucl. Chem. 299, 643–649. https://doi.org/10.1007/s10967-013-2774-6.

Poliakova, Tatiana R., Vlasova, Irina E., Kalmykov, Stepan N., 2024. Imaging Plate Radiography for Non-Destructive Determination of the Radioactivity Fraction in 'Hot' Particles. Nucl. Instrum. Methods Phys. Res., Sect. A 1065 (April), 169555. https://doi.org/10.1016/j.nima.2024.169555.

Porfiriev, B.N., 1996. Environmental Aftermath of the Radiation Accident at Tomsk-7. Environ. Manag. 20 (1), 25–33. https://doi.org/10.1007/PL00006699.

Powell, Brian A., Dai, Zurong, Zavarin, Mavrik, Zhao, Pihong, Kersting, Annie B., 2011. Stabilization of Plutonium Nano-Colloids by Epitaxial Distortion on Mineral Surfaces. Environ. Sci. Technol. 45 (7), 2698–2703. https://doi.org/10.1021/es1033487.

Quinto, Francesca, Hrnecek, Erich, Krachler, Michael, Shotyk, William, Winkler, Stephan R., 2013. Determination of 239Pu, 240Pu, 241Pu and 242Pu at Femtogram and Attogram Levels – Evidence for the Migration of Fallout Plutonium in an Ombrotrophic Peat Bog Profi Le. Environ Sci Process Impacts 15, 839–847. https://doi.org/10.1039/c3em30910j.

Romanchuk, Anna, Alexander Egorov, Yan Zubavichus, Andrei Shiryaev, Stepan Kalmykov, 2013. Formation of crystalline PuO2+x·nH2O nanoparticles upon sorption of Pu(V,VI) onto Hematite. Geochim. Cosmochim. Acta 121, 29–40.

Romanchuk, et al., 2016. Behavior of plutonium in the environment. Russ. Chem. Rev. 85 (9), 995–1010. https://doi.org/10.1070/rcr4602.

Santschi, P.H., Xu, C., Zhang, S., Schwehr, K.A., Grandbois, R., Kaplan, D.I., Yeager, C.M., 2017. Applied geochemistry iodine and plutonium association with natural organic matter : a review of recent advances *, 85, 121–127. https://doi.org/10.1016/j.apgeochem.2016.11.009.

Sokolik, G.A., Ovsiannikova, S.V., Ivanova, T.G., Leinova, S.L., 2004. Soil-Plant Transfer of Plutonium and Americium in Contaminated Regions of Belarus after the Chernobyl Catastrophe. Environ. Int. 30 (7), 939–947. https://doi.org/10.1016/j.envint.2004.03.003.

Tasi, Agost, Gaona, Xavier, Fellhauer, David, Böttle, Melanie, Rothe, Jörg, Dardenne, Kathy, Schild, Dieter, et al., 2018. Redox Behavior and Solubility of Plutonium under Alkaline, Reducing Conditions. Radiochim. Acta 106 (4), 259–279. https://doi.org/10.1515/ract-2017-2870.

Tcherkezian, V., Galushkin, B., Goryachenkova, T., Kashkarov, L., Liul, A., Roschina, I., Rumiantsev, O., 1995. Forms of Contamination of the Environment by Radionuclides after the Tomsk Accident (Russia, 1993). J. Environ. Radioact. 27 (2), 133–139. https://doi.org/10.1016/0265-931X(95)00014-2.

Testa, C., Jia, G., Degetto, S., Desideri, D., Guerra, F., Meli, M.A., Roselli, C., 1999. Vertical Profiles of 239,240Pu and 241Am in Two Sphagnum Mosses of Italian Peat. Sci. Total Environ. 232 (1–2), 27–31. https://doi.org/10.1016/S0048-9697(99)00106-0.

The Radiological Accident in the Reprocessing Plant at Tomsk, 1998. International Atomic Energy Agency, Vienna.

Toropov, A., Habarova, M., Rodionova, A., 2025. Organically bound species of rare earth and radioactive elements in terrestrial peat. Bull. Tomsk Polytech. Univ. Geo Assets Eng. 336 (10), 222–238. https://doi.org/10.18799/24131830/2025/10/4913.

Vosel, Yulia, Vosel, Sergey, Melgunov, Mikhail, Lazareva, Elena, Kropacheva, Marya, Strakhovenko, Vera, 2019. Discussions on the Driving Mechanism of Postdepositional Migration of 241Am and 137Cs in Organomineral Sediments (Lake Krugloe, Tomsk Region, Russia). Environ. Sci. Pollut. Res. 26 (19), 19180–19188. https://doi.org/10.1007/s11356-019-04726-w.

Walther, Clemens, Denecke, Melissa A., 2013. Actinide Colloids and Particles of Environmental Concern. Chem. Rev. 113 (2), 995–1015. https://doi.org/10.1021/cr300343c.

Wasserman, Naomi L., Merino, Nancy, Coutelot, Fanny, Kaplan, Daniel I., Powell, Brian A., Kersting, Annie B., Zavarin, Mavrik, 2023. Sources, seasonal cycling, and fate of plutonium in a seasonally stratified and radiologically contaminated pond. Sci. Rep. 13 (1), 1–12. https://doi.org/10.1038/s41598-023-37276-w.

World Reference Base for Soil Resources, 2022. International Soil Classification System for Naming Soils and Creating Legends for Soil Maps. https://doi.org/10.1002/jpln.202200417.

Xu, Chen, Zhang, Saijin, Kaplan, Daniel I., Ho, Yi Fang, Schwehr, Kathleen A., Roberts, Kimberly A., Chen, Hongmei, et al., 2015. Evidence for hydroxamate siderophores and other N-containing organic compounds controlling 239,240Pu immobilization and remobilization in a wetland sediment. Environ. Sci. Technol. 49 (19), 11458–11467. https://doi.org/10.1021/acs.est.5b02310.

Yakovlev, Evgeny, Spirov, Ruslan, Druzhinin, Sergey, Ocheretenko, Alina, Druzhinina, Anna, Mishchenko, Egor, 2021. Atmospheric fallout of radionuclides in peat bogs in the western segment of the Russian Arctic. Environ. Sci. Pollut. Res. 28, 25460–25478.

Zavarin, Mavrik, Zhao, Pihong, Dai, Zurong, Kersting, Annie B., 2014. Plutonium sorption and precipitation in the presence of Goethite at 25 and 80°C. Radiochim. Acta 102 (11), 983–997. https://doi.org/10.1515/ract-2013-2188.

Zhao, Pihong, Zavarin, Mavrik, Leif, Roald N., Powell, Brian A., Singleton, Michael J., Lindvall, Rachel E., Kersting, Annie B., 2011. Mobilization of Actinides by Dissolved Organic Compounds at the Nevada Test Site. Appl. Geochem. 26 (3), 308–318. https://doi.org/10.1016/j.apgeochem.2010.12.004.

Zhao, Pihong, Zavarin, Mavrik, Dai, Zurong, Kersting, Annie B., 2020. Stability of plutonium oxide nanoparticles in the presence of montmorillonite and implications for colloid facilitated transport. Appl. Geochem. 122 (May), 104725. https://doi.org/10.1016/j.apgeochem.2020.104725.

Zhao, Xue, Hou, Xiaolin, Huang, Zhao, Tang, Lu, 2024. Source, preservation and re-suspension of 239,240Pu in a well dated core collected from Northwest China. Chemosphere 359, 142267. https://doi.org/10.1016/j.chemosphere.2024.142267.